J Eng Math
DOI 10.1007/s10665-010-9427-3

Preface to the fifth special issue on practical asymptotics

A. Korobkin

Ten years ago the first *Special Issue on Practical Asymptotics* was published by the Journal of Engineering Mathematics [1]. Professor H.K. Kuiken was the editor of that Issue. He wrote in the Preface "... these days applied mathematics seems, at first sight anyway, to become more and more dominated by direct numerical simulations. Admittedly, this leads to new insights which, it would seem, could not have been attained by other means" and "... many believe that asymptotics deals with exceptional cases which are usually outside the practical domain. However, this is a misconception!" The Guest-Editors of the following, second, third and fourth issues on practical asymptotics, argued that asymptotic solutions and asymptotic methods remain and will be valuable because they "provide important complements to numerical simulation" [2], "can offer ways to systematically study problems that may otherwise be inaccessible" [3] and "may provide quantitative and/or qualitative information that computer simulations can not" [4]. It is seen that the issues on practical asymptotics are a forum for discussion "Does the asymptotic analysis have a future in the era of supercomputers?". The answer to the question is obvious: "Yes, it has."

Researchers and engineers, who use asymptotic methods and/or approximations inspired by these methods to solve *practical* problems, well understand that asymptotic analysis is a powerful tool, the range of applicability of which is very wide but does not cover everything we need. However, the situation is not so simple. There is a difficulty which is not about the application of asymptotic methods to practical problems but about the "public" opinion that asymptotic and, in general, mathematical tools are "old-fashioned" compared with direct numerical simulations. These days even academics sometimes ask the question "Why do we need this complicated analysis, if the problem can be easily solved by computer simulations?"

Before the 90s numerical calculations were complementary to rigorous or approximate analysis of a problem. At the present time the "center of mass" in research is still moving towards computations. However, along this way, it is getting more and more clear that computer simulations being applied to practical problems is not a universal panacea. Euphoria about computers is still high but a more practical point of view is becoming at least visible these days: computation is a research tool as are many other approximate or rigorous tools of mathematics which help us to gain new knowledge, understand important phenomena and solve challenging practical problems.

It would be perfect if our problems could be solved in a rigorous way. But this is an ideal situation which happens quite rarely, especially in new formulations. In order to obtain a solution, we need rigorous mathematical methods, approximate methods, with asymptotic methods being the most powerful of them, and computations. It is wrong

A. Korobkin (✉)
University of East Anglia, Norwich, UK
e-mail: a.korobkin@uea.ac.uk

Published online: 17 November 2010

for any of these methods to claim that it is superior and all others can be well forgotten. We need all means and their proper combinations to help us to approximate the solution. This is a practical approach to practical problems. There is a long way ahead before this balanced approach will be widely adopted. The series of *Special Issues on Practical Asymptotics* initiated by Professor H.K. Kuiken plays an important role in this process, stressing the practical importance of asymptotic methods in the analysis of real-life problems.

Working as a Guest Editor on the *Practical Asymptotics—V* issue helped me to recognize that asymptotic analysis is a practical research tool not only in my area of fluid-structure interaction but in many other areas ranging from chemistry to water waves. This task helped me also to recognize that we are missing rigorous mathematical tools in practical research. They are much less present in practical research than asymptotic methods nowadays. Without such tools we are missing a rigorous background which must give us a certain measure of security.

The present issue is special because we invited many Ukrainian and Russian researchers to contribute. There are no papers in this issue from Ukraine but this is not because outstanding scientists from that country were not approached. Four papers out of 10 in this issue are from Russia, and 6 out of 10 are by Russian-speaking authors. One reason why the journal pays special attention to these two countries is well explained in the Preface to the Special Issue "A Taste of Engineering Mathematics from Present-day Russia" published by the journal in 2006 [5].

The present issue is concerned with body motion in a two-layer fluid [6], interaction of water waves with a porous plate [7], displacement of one fluid by another in a porous medium [8], liquid-film flows over a step topography with external electric field [9], turbulent flows produced on rotating blades [10], a water-impact problem [11], the Maslov canonical operator for shallow-water equations with localized initial data [12], internal gravity waves over a bottom topography [13], a reaction—diffusion model for concrete corrosion in sewer pipes [14] and convection in a two-layer fluid with external high-frequency vibration [15]. Different methods of asymptotic analysis such as the homogenization method, the Maslov canonical operator, the method of matched asymptotic expansions, generalized methods from geometric optics, and their combinations with numerical methods are used to demonstrate their practical importance in the analysis of practical problems.

References

1. Kuiken HK (2001) Practical asymptotics. J Eng Math 39:1–2
2. Holmes MH, King JR (2003) Introduction. J Eng Math 45:1–2
3. Witelski TP, Rienstra SW (2005) Introduction to practical asymptotics III. J Eng Math 53:199
4. McCue SW (2009) Preface to fourth special issue on practical asymptotics. J Eng Math 63:153–154
5. Korobkin A (2006) A taste of engineering mathematics from present-day Russia. J Eng Math 55:1–8
6. Motygin O, Kuznetsov N (2011) On the forward motion of an interface-crossing body in a two-layer fluid: the role of asymptotics in the problems statement. J Eng Math 69:113–134
7. Evans DV, Peter MA (2011) Asymptotic reflection of linear water waves by submerged horizontal porous plates. J Eng Math 69:135–154
8. Booth RJS (2011) Asymptotics for the Muskat problem. J Eng Math 69:155–168
9. Tseluiko D, Blyth MG, Papageorgiou DT, Vanden-Broeck JM (2011) Electrified film flow over step topography at zero Reynolds number: an analytical and computational study. J Eng Math 69:169–184
10. McDarby JM, Smith FT (2011) Turbulent interactions for rotating blades and wakes. J Eng Math 69:185–198
11. Iafrati A, Korobkin A (2011) Asymptotic estimates of hydrodynamic loads in the early stage of water entry of a circular disk. J Eng Math 69:199–224
12. Dobrokhotov SYu, Nekrasov RV, Tirozzi B (2011) Asymptotic solutions of the linear shallow water equations with localized initial data. J Eng Math 69:225–242
13. Bulatov VV, Vladimirov YuV (2011) The uniform asymptotic form of the internal gravity-wave field generated by a source moving above a smoothly varying bottom. J Eng Math 69:243–260
14. Fatima T, Arab N, Zemskov EP, Muntean A (2011) Homogenization of a reaction—diffusion system modeling sulfate corrosion of concrete in locally periodic perforated domains. J Eng Math 69:261–276
15. Zenkovskaya SM, Novosiadliy VA (2011) Averaging method and long-wave asymptotics in vibrational convection in layers with an interface. J Eng Math 69:277–290

J Eng Math
DOI 10.1007/s10665-010-9388-6

The uniform asymptotic form of the internal gravity-wave field generated by a source moving above a smoothly varying bottom

Vitaly V. Bulatov · Yury V. Vladimirov

Received: 27 May 2009 / Accepted: 2 July 2010

Abstract The uniform asymptotic form of the internal gravity-wave field generated by a source moving above a smoothly varying bottom is constructed. The problem of reconstructing non-harmonic internal gravity-wave packets generated by a source moving in a stratified ocean is considered. The solution is proposed in terms of wave modes, propagating independently at the adiabatic approximation, and described as a non-integral-degree series of a small parameter characterizing the stratified medium. A specific form of the wave packets, which can be parameterized in terms of model functions (Airy functions), depends on the local behavior of the dispersion curves of the individual wave mode. A modified space–time ray method was proposed, which belongs to the class of geometrical-optics methods. The key point of the proposed technique is the possibility to derive the asymptotic representation of the solution in terms of a non-integral-degree series of the some small parameter.

Keywords Caustic surface · Eikonal equation · Rays and wave fronts · Stratified medium · WKB approximation

1 Introduction

Internal gravity waves are oscillations of a stratified medium in a gravity force field. In a stratified medium the density increases with the depth. Suppose that a volume element of the medium is not at equilibrium, for example it could be displaced upward, then it will be heavier than the surrounding medium and therefore Archimedean forces will cause it to move back to equilibrium. The essential parameter of any oscillating system is the frequency. It is determined by the correlation of two factors: returning forces which return the perturbed system towards its equilibrium and inertial forces. For internal gravity waves the returning forces are proportional to the vertical gradient of the fluid's density and the inertial ones are proportional to the density itself. For the characteristic frequency of gravity-wave oscillations we have the following expression: $N^2(z) = -\frac{g}{\rho(z)}\frac{\mathrm{d}\rho(z)}{\mathrm{d}z}$ [6, Chap. 1]. This frequency is usually called by the Brunt–Vaisala frequency or the buoyancy frequency [15, Chaps. 1, 2]. Here $\rho(z)$ is the density considered as a function of the depth z, g is the acceleration in the gravity force field, the sign "$-$" originates from the increase of the density with the depth and therefore $\frac{\mathrm{d}\rho(z)}{\mathrm{d}z} < 0$ [12, Chap. 4].

The exact solutions of the essential equations describing internal gravity waves are only obtained for special cases [3, Chaps. 2–9]. That is the reason why the approximate asymptotic methods are systematically used for the

V. V. Bulatov (✉) · Y. V. Vladimirov
Institute for Problems in Mechanics, Russian Academy of Sciences, Pr. Vernadskogo 101-1, 119526 Moscow, Russia
e-mail: bulatov@index-xx.ru

Published online: 20 July 2010

investigation of internal gravity-wave fields in a stratified ocean. Internal gravity waves are usually represented in the following integral form [3, Chaps. 1, 2], [8,17]: $J = \int_\gamma \exp[\lambda f(z)]\, F(z)\mathrm{d}z, \quad \lambda >> 1$, where $f(z)$ and $F(z)$ are analytic functions of the complex variable $N^2(z)$; L_z is a contour of integration in the complex plane $\delta = \frac{N^2 L_z}{g}$. The universal way to construct the asymptotic forms of such integrals is the method of etalon integrals [1, Chap. 1], [2, Chaps. 1, 3, 5].

This paper is devoted to the systematic description of a generalization of the geometrical-optics method, i.e., we discuss the spatio-temporal ray method of etalon functions [1, Chap. 2]. This method allows one to solve the problem of asymptotic modeling of the inharmonic wave packet's dynamics for internal gravity waves in stratified media with slowly varying parameters. The main reasons to use ray method are the following: the ray representations are well correlated with intuition and with the empirical material for the propagation of the internal gravity waves in natural stratified media (ocean, atmosphere). These methods are universal and very often one can use only these for the approximate computations of wave fields in slowly changing non-homogeneous stratified media [1, Chap. 3].

The horizontal non-homogeneity and non-stationarity are crucial for the propagation of internal gravity waves in natural stratified media (such as the ocean and the atmosphere). To the most typical horizontal inhomogeneities of the real ocean we reckon changes in the ocean bottom shape, inhomogeneities of the density field and the variance of the mean currents. The exact solution of the problem, for example by means of separating of variables, can only be obtained when the density distribution and the ocean-bottom shape are described by simple model functions. For arbitrary stratification and arbitrary ocean-bottom topography it is only possible to construct asymptotic representations of the solutions [9–11,14,16,18].

However, if the depth or the ocean and its density vary slowly in comparison with the characteristic length (period) of the internal gravity waves, which occur in the real ocean, then one can use the spatio-temporal ray method (the geometrical-optics method) and its generalizations to investigate the mathematically modeled dynamics of internal gravity waves. In [6, Chaps. 3, 8, 9] asymptotic forms of the internal gravity-wave far field were obtained for the case of constant depth. It was also shown that the far field is equal to the sum of modes, each of the modes being confined within its Mach cone. One can represent the asymptotic form of each mode via Airy functions (Airy wave) or the Fresnel integrals (Fresnel wave).

One can solve the problem using the modified spatio-temporal ray method (the geometrical-optics method) proposed above. This is the method of etalon functions [1, Chaps. 2, 3]. Its distinguishing feature is that, in order to investigate the evolution of non-harmonic wave packets in stratified non-stationary horizontally non-homogeneous media, one seeks solution in the form of a rational power series with respect to the small parameter. The powers depend on the form of representation for the wave packet. The form of representation is determined by the asymptotic behavior of the solution in the stationary horizontally homogeneous case [6, Chap. 3]. The phase of the wave packet can be obtained from the corresponding eikonal equation, which can be solved numerically on the characteristics (rays). The amplitude of the wave packet can be found from a conservation law along the characteristics (rays) [1, Chap. 2], [4,5].

The slowness condition of the change in parameters of the medium in time and along the horizontal is crucial for applying geometrical-optics methods. The slowness is considered in comparison with the characteristic lengths and periods of internal gravity waves. However, these conditions are not sufficient for geometrical-optics methods to be valid. It is clear that to estimate the accuracy of the geometrical-optics method one has to use results obtained by a more precise approach than that of the spatio-temporal ray method. However, because of the serious mathematical difficulties involved, this is not yet possible. For the investigation of the dynamics of inharmonic internal gravity-wave packets in stratified non-homogeneous and non-stationary media, we have available analytic methods which are limited and do not allow one to estimate the accuracy of the geometrical-optics method for real media. In the general case there are no exact solutions, and the known rigorous solutions just indicate a possible value of inaccuracy for typical cases. The same results for the level of inaccuracy of the spatio-temporal ray method can be obtained by comparing the asymptotic results with the approximate level (but more general than that of the ray method) solutions of the basic wave problems. Therefore, the validity of the spatio-temporal method and of its results follows from a comparison of the results with data from natural experiments [6, Chap. 5].

Investigating the evolution of internal gravity wave packets in stratified media with slowly varying parameters, one usually assumes that the packet is locally harmonic. In contrast to most of the works devoted to the subject, the modified geometrical-optics method of etalon functions elaborated here, and its modifications in the form of decomposition into some special functions, gives an opportunity to describe the structure of the wave fields near and far from wave fronts [4,8,17].

By using one of the modifications of the geometrical-optics method one solves the problem of constructing a uniform asymptotic form for the far field in the case of a smoothly varying bottom. This is done by use of asymptotic representations of the wave field for large distances from the source in the case of constant bottom topography. We call such a modification "vertical modes–horizontal rays" [1, Chap. 4]. In this method one does not assume that there is slowness in the vertical direction. The solutions are represented as an expansion in waves of a special form, Airy waves. These describe not only the evolution of non-harmonic wave packets when these propagate above a slowly transforming ocean bottom but also the structure of the wave field of each particular mode either close to or far from the wave fronts of the modes. The argument of each Airy wave is determined by the solution of the corresponding eikonal equation. The amplitude of the wave field is obtained from the energy-conservation law along the ray tube [4,5], [6, Chap. 3].

The exact analytical expressions for the rays are obtained and the features of the phase structure for the wave field are analyzed for model forms of the stratification and the bottom shape, describing the typical structure of the ocean shelf. It is shown, in particular, that different features of wave-field structures can be displayed depending on the trajectory of the source, the ocean bottom shape and its stratification. The "blocking" spatial effect with respect to the low-frequency modes of the wave field generated by the source moving along the shore of the ocean with an overcritical velocity is analyzed.

2 Main equations

Let us consider a non-viscous incompressible non-homogeneous liquid. If it is unperturbed, we denote its density by $\rho_0(z)$ (the stratification is supposed to be stable, i.e, $\rho_0'(z) < 0$, the axis z is directed downward from the liquid's surface).

The system of hydrodynamic equations takes the following form [12, Chap. 4], [15, Chap. 1]:

$$\frac{\partial \mathbf{v}}{\partial t} + (\mathbf{v}\cdot\nabla)\mathbf{v} = -\frac{\nabla p}{\rho} + \mathbf{g}, \quad \operatorname{div}\mathbf{v} = 0, \quad \frac{\partial \rho}{\partial t} + \nabla\rho\cdot\mathbf{v} = 0.$$

The linearized system can be expressed as follows [3, Chap. 2], [6, Chap. 1]:

$$u_t' + \frac{1}{\rho_0(z)}p_x' = 0, \quad v_t' + \frac{1}{\rho_0(z)}p_y' = 0, \quad w_t' + \frac{1}{\rho_0(z)}p_z' + g\frac{\rho}{\rho_0(z)} = 0, \quad u_x' + v_y' + w_z' = 0, \quad \rho_t' + \rho_{0_z}'\cdot w = 0, \tag{2.1}$$

where $\mathbf{v} = (u, v, w)$ is the velocities' vector, $\mathbf{g} = (0, 0, g)$ is the gravitational acceleration vector, p and ρ are the deviations of the pressure and the density from their equilibrium values [4,7], [15, Chap. 1]. A general analysis of the system (2.1) allows to obtain the equation for the vertical component of the velocity [6, Chap. 1], [12, Chap. 4]

$$\Delta w_{tt} + w_{zztt} - \frac{N^2(z)}{g}w_{ztt} + N^2(z)\Delta w = 0, \quad \Delta = \frac{\partial^2}{\partial x^2} + \frac{\partial^2}{\partial y^2}, \quad N^2(z) = -\frac{g}{\rho_0(z)}\rho_0'(z), \tag{2.2}$$

where $N^2(z)$ is the Brunt–Vaisala frequency. Let us estimate the third equation from (2.2) in comparison with the second one. If we introduce the characteristic vertical scale L_z, then the ratio of the third equation to the second one is

$$\delta = \frac{N^2 L_z}{g}.$$

If $\delta << 1$ (in the real ocean one has $\delta \sim 10^{-2}$), then (2.2) becomes

$$\Delta w_{tt} + w_{zztt} + N^2(z)\Delta w = 0 \tag{2.3}$$

and the corresponding approximation is called the Boussinesq approximation [15, Chaps. 1, 2].

It is interesting to note that when $N^2(z) = N^2 = \text{const}$ and when the depth H is constant, then

$$\delta = \frac{N^2 H^2}{gH} = \frac{\pi^2 c_{\max}^2}{c^2}.$$

Here $c = \sqrt{gH}$ is the velocity of long waves on a surface of liquid with depth H [3, Chap. 3], and $c_{\max} = NH/\pi$ is the maximum group velocity of the internal waves. In the real ocean one has $c \sim 100$ m/s, and $c_{\max} \sim 1$ m/s [15, Chap. 3], [16]. From system (2.1) it is possible to obtain that the horizontal components of velocity, u and v, are coupled to the vertical component by the ratio [4], [6, Chap. 1]

$$\frac{\partial}{\partial t}(\Delta v + w_{zy}) = 0, \quad \frac{\partial}{\partial t}(\Delta u + w_{zx}) = 0.$$

3 The equations of internal gravity waves for a moving point-mass source

Let us consider a layer in the liquid with Brunt–Vaisala frequency $N(\tilde{z})$. Let this layer be bounded by the surface $\tilde{z} = 0$ and the bottom $\tilde{z} = \tilde{H}(\tilde{x}, \tilde{y})$. Let the point-mass source with intensity Q (here Q is the volume discharge per second) moves at depth $\tilde{z}_0$ uniformly and rectilinearly with the velocity V in the negative direction of the abscissa.

Now the velocity field in the Boussinesq approximation satisfies the following system of equations [6, Chap. 1]

$$\begin{gathered}
\frac{\partial^2}{\partial t^2}\left(\Delta\tilde{w} + \frac{\partial^2}{\partial\tilde{z}^2}\tilde{w}\right) + N^2(\tilde{z})\Delta\tilde{w} = Q\delta''_{tt}(\tilde{x} + Vt)\delta(\tilde{y} - \tilde{y}_0)\delta'(\tilde{z} - \tilde{z}_0), \\
\Delta\tilde{u} + \frac{\partial^2\tilde{w}}{\partial\tilde{\xi}\partial\tilde{z}} = Q\delta'(\tilde{\xi})\delta(\tilde{y} - \tilde{y}_0)\delta(\tilde{z} - \tilde{z}_0), \quad \Delta\tilde{v} + \frac{\partial^2 w}{\partial\tilde{y}\partial\tilde{z}} = Q\delta(\tilde{\xi})\delta'(\tilde{y} - \tilde{y}_0)\delta(\tilde{z} - \tilde{z}_0), \qquad (3.1) \\
\Delta = \frac{\partial^2}{\partial\tilde{\xi}^2} + \frac{\partial^2}{\partial\tilde{y}^2}, \quad \tilde{\xi} = \tilde{x} + Vt.
\end{gathered}$$

At the layer's boundaries the following conditions should be satisfied [10,11,14,18]:

$$\begin{gathered}
\tilde{w} = 0 \quad \text{at } \tilde{z} = 0, \\
\tilde{w} = \tilde{u}\frac{\partial\tilde{u}}{\partial\tilde{x}} + \tilde{v}\frac{\partial\tilde{H}}{\partial\tilde{y}} \quad \text{at } \tilde{z} = \tilde{H}(\tilde{x}, \tilde{y}). \qquad (3.2)
\end{gathered}$$

Further we consider the case when $N = \text{const}$, $\tilde{H}(\tilde{y}) = \beta\tilde{y}$ (i.e., when the depth depends linearly on the coordinate $\tilde{y}$, and the source moves along the line $\tilde{z} = \tilde{z}_0$, $\tilde{y} = \tilde{y}_0$).

Introducing the horizontal scale

$$L_y = L_\xi = \frac{V}{N}\frac{\pi}{\beta} = \frac{V}{N}\lambda \quad \left(\lambda = \frac{\pi}{\beta}, \lambda >> 1\right)$$

and the vertical scale $L_z = \frac{V}{N}y_0$, we have the following relations between the non-dimensional coordinates and the dimensional ones

$$\begin{gathered}
\xi = \tilde{\xi}\frac{N}{V\lambda}, \quad y = \tilde{y}\frac{N}{V\lambda}, \quad z = \tilde{z}\frac{N}{Vy_0}; \quad H(y) = \frac{\pi y}{y_0}, \\
(u, v, w) = \frac{(\tilde{u}, \tilde{v}, \tilde{w})V^2}{QN^2}.
\end{gathered}$$

We note that $y = 1/M$, where M is the Mach number $M = V/c_{\max}$, and $c_{\max}$ is the maximum value of the group velocity for the internal gravity waves $c_{\max} = \frac{N\tilde{H}(\tilde{y})}{\pi} = Vy$ [6, Chaps. 1, 2].

Thus, the domain $y < 1$ corresponds to $M > 1$ (i.e., the velocity of the source is greater than $c_{\max}$), and the domain $y > 1$ corresponds to $M < 1$ (i.e., $c_{\max}$ is greater than the velocity of the source V).

In non-dimensional coordinates the system of equations (3.1) and the system of boundary conditions (3.2) take the forms

$$\frac{\partial^2}{\partial\xi^2}\left(\frac{1}{\lambda^2}\Delta+\frac{1}{y_0^2}\frac{\partial^2}{\partial z^2}\right)w+\Delta w=\frac{1}{\lambda^2 y_0^2}\delta''_{\xi\xi}(\xi)\delta(y-y_0)\delta'_z(z-z_0),$$

$$\frac{1}{\lambda}\Delta v+\frac{1}{y_0}\frac{\partial^2 w}{\partial y\partial z}=\frac{1}{\lambda^2 y_0}\delta(\xi)\delta'(y-y_0)\delta(z-z_0),\quad \frac{1}{\lambda}\Delta u+\frac{1}{y_0}\frac{\partial^2 w}{\partial\xi\partial z}=\frac{1}{\lambda^2 y_0}\delta'(\xi)\delta(y-y_0)\delta(z-z_0), \tag{3.3}$$

$$w=0\quad \text{at } z=0,$$

$$w=\frac{\pi}{\lambda}v\quad \text{at } z=H(y). \tag{3.4}$$

Since the boundary conditions (3.4) do not depend on the horizontal velocity, the system (3.3) splits into two first equations and a separated third one. If the two first equations are solved, the function u can be easily obtained from the third equation.

We look for the solutions of the first two equations of system (3.3) in the form of a sum of wave modes [5], [6, Chap. 3]

$$w=\sum_{n=1}^{\infty}w^n,\quad v=\sum_{n=1}^{\infty}v^n.$$

Further we consider only the dominant (first) mode omitting the upper index n. We seek a solution of the form [1, Chap. 2]

$$w=\int F(z,y,\omega)\mathrm{e}^{\mathrm{i}\lambda(\omega\xi-s(y,\omega))}\mathrm{d}\omega,\quad v=\int \Psi(z,y,\omega)\mathrm{e}^{\mathrm{i}\lambda(\omega\xi-s(y,\omega))}\mathrm{d}\omega, \tag{3.5}$$

where

$$F=F_0(z,y,\omega)+\frac{\mathrm{i}}{\lambda}F_1(z,y,\omega)+O\left(\frac{1}{\lambda^2}\right),\quad \Psi=\mathrm{i}\Psi_1(z,y,\omega)+O\left(\frac{1}{\lambda}\right)$$

We emphasize that the functions w and v depend on ξ only via the phases of elementary solutions, superposition of which gives the complete solutions F and Ψ. Therefore the problem is reduced to finding functions $F(z,y,\omega)$ and $s(y,\omega)$.

Let us substitute w and v from (3.5) in the first two equations of (3.3) and in the boundary conditions (3.4); then equate the members at the corresponding powers of λ [6, Chap. 3]. In this way we obtain two equations for the functions $F_0(z,y,\omega)$ and $F_1(z,y,\omega)$:

$$F''_{0_{zz}}+\frac{\omega^2+s'^2_y}{\omega^2}\left(1-\omega^2\right)y_0^2F_0=0,\quad F_0|_{z=0}=0,\quad F_0|_{z=H(y)}=0, \tag{3.6}$$

$$F''_{1_{zz}}+\frac{\omega^2+s'^2_y}{\omega^2}\left(1-\omega^2\right)y_0^2F_1=\frac{\left(1-\omega^2\right)y_0^2}{\omega^2}\left(2F'_{0_y}s'_y+F_0s''_{yy}\right),\quad F_1|_{z=0}=0,\ F_1|_{z=H(y)}$$

$$=-\frac{\pi s'_y}{y_0(\omega^2+s'^2_y)}F'_{0_z}. \tag{3.7}$$

Let us consider the Sturm–Liouville problem (3.6). The quantification condition yields (we remind that the dominant mode is considered, i.e. $n=1$) [15, Chap. 4]:

the eikonal equation

$$\omega^2+s'^2_y(y,\omega)=k^2(\omega,y);$$

the dispersion relation

$$k^2(\omega,y)=\frac{\omega^2}{\left(1-\omega^2\right)y^2};$$

and the eigenfunction $F_0(z,y,\omega)=c(y,\omega)\sin\frac{zy_0}{y}$, where $c(y,\omega)$ is yet an arbitrary function which does not depend on z.

4 Finding the factor $c(y, \omega)$ from the conservation law and the locality principle

In order to find out how the function $c(y, \omega)$ depends on y we multiply (3.7) by F_0 and then integrate the result by z from 0 to $H(y)$. Integration by parts of the left-hand part yields

$$F'_{0z}\big|_{z=H(y)} \cdot \frac{\pi s'_y(y,\omega)}{y_0 k^2(y,\omega)} = -\frac{1-\omega^2}{\omega^2} y_0^2 \int\limits_0^{H(y)} \frac{\partial}{\partial y}\left(s'_y F_0^2\right) \mathrm{d}z, \tag{4.1}$$

where

$$\int\limits_0^{H(y)} \frac{\partial}{\partial y}\left(s'_y F_0^2\right) \mathrm{d}z = \frac{\partial}{\partial y}\left(s'_y \Phi\right), \quad \Phi = \int\limits_0^{H(y)} F_0^2 \mathrm{d}z = C^2(y,\omega)\frac{\pi}{2} \cdot \frac{y}{y_0}. \tag{4.2}$$

In order to find $F'_{0_z}\Big|_{z=H(y)}$ from the left-hand member of (4.1), we differentiate (3.6) by y, multiply the result by F_0 and then integrate by parts from 0 to $H(y)$. Hence we obtain

$$y_0^2 \cdot \frac{1-\omega^2}{\omega^2}\frac{\partial}{\partial y}\left(k^2(y,\omega)\right)\Phi + F'_{0_z}\Big|_{z=H(y)} \frac{\partial H}{\partial y} = 0.$$

From here it follows

$$\frac{\pi}{y_0}\frac{s'_y}{k^2}\, F'_{0_z}\Big|_{z=H(y)} = -y_0^2 \frac{1-\omega^2}{\omega^2}\frac{\partial k^2}{\partial y}\Phi\frac{s'_y}{k^2} \tag{4.3}$$

Substituting (4.3) and (4.2) in (4.1) yields

$$\Phi s'_y \left(\log k^2\right)'_y = \frac{\partial}{\partial y}(s'\Phi).$$

The equation $\frac{s'_y \Phi}{k^2(y,\omega)} = \mathrm{const}(\omega, y_0)$ is the conservation law [6, Chap. 3].

Rewriting the conservation law as

$$\frac{s'_y(y,\omega)\frac{\pi}{2}\frac{y}{y_0}c^2(y,\omega)}{k^2(y,\omega)} = \frac{s'_y(y_0,\omega)\frac{\pi}{2}c^2(y_0,\omega)}{k^2(y_0,\omega)},$$

we find

$$c(y,\omega) = c(y_0,\omega)\frac{y_0}{y}\sqrt[4]{\frac{1-\left(1-\omega^2\right)y_0^2}{1-\left(1-\omega^2\right)y^2}}.$$

Using the locality principle, i.e. the known solution of the problem for the constant depth $H(y_0) = \pi$ [4,5], we determine $c(y_0, \omega)$in the form

$$c(y_0,\omega) = \frac{2\mathrm{i}\omega \sin z_0}{\pi\sqrt{1-\omega^2}\sqrt{1-\left(1-\omega^2\right)y_0^2}}.$$

Finally we have

$$F_0(y,\omega,z) = \frac{2\mathrm{i}}{\pi}\frac{y_0}{y}\frac{\omega}{\sqrt{1-\omega^2}}\frac{\sin z_0 \ \sin\left(\frac{zy_0}{y}\right)}{\sqrt[4]{1-\left(1-\omega^2\right)y^2}\sqrt[4]{1-\left(1-\omega^2\right)y_0^2}}. \tag{4.4}$$

5 The field in the domain of the subcritical velocity ($y < 1$); rays and the stationary phase method

Let us consider the eikonal equation

$$s_y'^2(y,\omega) = \frac{\omega^2}{\left(1-\omega^2\right)y^2} - \omega^2.$$

From here we get

$$s(y,\omega) = \int_{y_0}^{y} \frac{\omega\sqrt{1-y^2\alpha}}{y\sqrt{\alpha}}\mathrm{d}y = \frac{\omega}{\sqrt{\alpha}}\left(\left(\sqrt{1-y^2\alpha} - \log\left(1+\sqrt{1-y^2\alpha}\right) + \log y\right)\right.$$
$$\left. - \left(\sqrt{1-y_0^2\alpha} - \log\left(1+\sqrt{1-y_0^2\alpha} + \log y_0\right)\right)\right), \tag{5.1}$$

$\alpha = 1-\omega^2$.

Then the field of the incident wave has the following form (in the domain $y_0 < y < 1$)

$$w = \int_0^1 \frac{4}{\pi}\frac{y_0}{y}\frac{\omega}{\sqrt{1-\omega^2}}\frac{\sin z_0 \ \sin\frac{zy_o}{y}}{\sqrt[4]{1-y^2\left(1-\omega^2\right)}\sqrt[4]{1-y_0^2\left(1-\omega^2\right)}}\cos\left(\lambda\left[\omega\xi - s(y,\omega)\right] + \frac{\pi}{2}\right)\mathrm{d}\omega. \tag{5.2}$$

To investigate the integral (5.2) at large values of λ by the stationary-phase method, we introduce the family of rays. We define it as the set of points at which the phase $\chi(\omega,\xi,y) = \lambda\left(\omega\xi - s(y,\omega)\right) + \frac{\pi}{2}$ is stationary, i.e., $\frac{\partial\chi(\omega,\xi,y)}{\partial\omega} = 0$ or $\xi(y,\omega) = \frac{\partial s(y,\omega)}{\partial\omega}$. Differentiating (5.1) by ω, we obtain the family of the desired rays:

$$\xi(y,\omega) = \frac{\alpha\sqrt{1-y^2\alpha} - \log\left(1+\sqrt{1-y^2\alpha}\right) + \log y - \alpha\sqrt{1-y_0^2\alpha} + \log\left(1+\sqrt{1-y_0^2\alpha}\right) - \log y_0}{\alpha^{3/2}}. \tag{5.3}$$

The expression (5.3) determines a one-parameter family of ascending rays on the plane ξ, y. These rays start at the point $\xi = 0$, $y = y_0$ with the parameter λ (or ω). At a certain value of ω we have a certain ray. However, the expression (5.3) describes the ray's behavior only before the turning point $y_* = \frac{1}{\sqrt{\alpha}}$, $\xi_* = \xi(y_*,\alpha)$ (i.e., at $\xi \le \xi_*$).

The reflected ray ($\xi \le \xi_*$) is constructed as follows. First we determine the eikonal of the reflected ray $s_1(y,\omega)$:

$$s_1(y,\omega) = s(y_*,\omega) - \int_{y_*}^{y}\frac{\omega\sqrt{1-y^2\alpha}}{y\sqrt{\alpha}}\mathrm{d}y$$
$$= \frac{\omega}{\sqrt{\alpha}}\left(\left(-\sqrt{1-y^2\alpha} + \log\left(1+\sqrt{1-y^2\alpha}\right) - \log y - \log\alpha\right)\right.$$
$$\left. - \left(\sqrt{1-y_0^2\alpha} - \log\left(1+\sqrt{1-y_0^2\alpha}\right) + \log y_0\right)\right) \tag{5.4}$$

Then for the reflected field w_1 in the whole domain $0 < y < 1$ we obtain the following expression:

$$w_1 = \int_0^1 \frac{4}{\pi}\frac{y_0}{y}\frac{\omega}{\sqrt{1-\omega^2}}\frac{\sin z_0 \ \sin\frac{zy_0}{y}}{\sqrt[4]{1-y^2\left(1-\omega^2\right)}\sqrt[4]{1-y_0^2\left(1-\omega^2\right)}}\cos\left(\lambda\left(\omega\xi - s_1(y,\omega)\right) + \pi\right)\mathrm{d}\omega, \tag{5.5}$$

i.e., in comparison with w instead of the eikonal of the incident wave $s(y,\omega)$ we use the eikonal of the reflected wave $s_1(y,\omega)$. The phase shift $(+\pi/2)$ due to the reflection of the ray is also taken into account. The reflected ray is constructed analogously to the incident one:

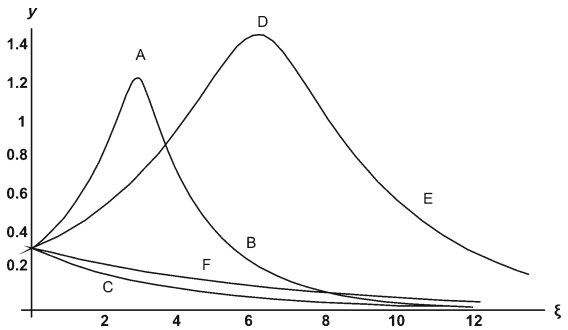

Fig. 1 Rays from a moving source for and $y_0 = 0.3$ and $\omega = 0.6$ (line AB, C), $\omega = 0.75$ (line DE, F)

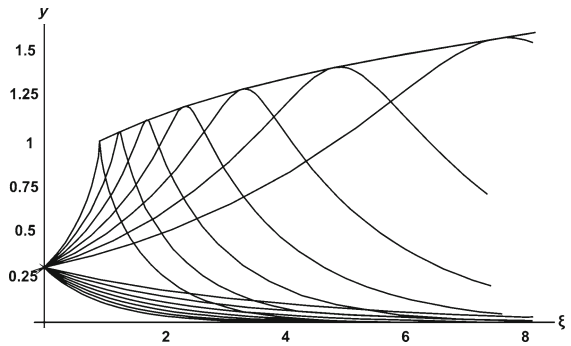

Fig. 2 Rays from a moving source for $y_0 = 0.3$, value of ω change from 0 to 0.77 with step 0.11

Fig. 3 Rays from a moving source for $y_0 = 0.6$, the value of ω change from 0 to 0.77 with step 0.07

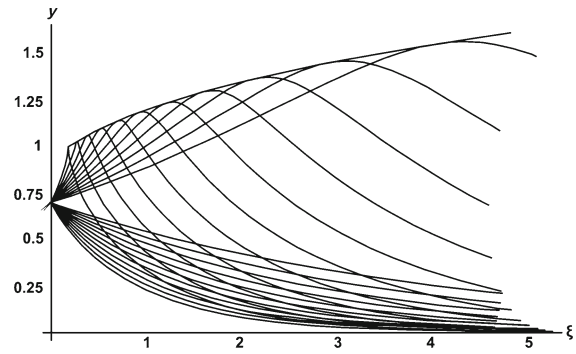

$$\xi_1(y,\alpha) = \frac{\partial s_1}{\partial \omega},$$

$$\xi_1(y,\alpha) = \frac{-\alpha\sqrt{1-y^2\alpha} + \log\left(1+\sqrt{1-y^2\alpha}\right) - \log y}{\alpha^{3/2}}$$

$$+\frac{-\alpha\sqrt{1-y_0^2\alpha} + \log\left(1+\sqrt{1-y_0^2\alpha}\right) - \log y_0 - \log\alpha}{\alpha^{3/2}}. \tag{5.6}$$

A comparison of (5.3) and (5.6) shows that the incident and the reflected rays are symmetric at $y_0 < y < 1$ with respect to the line $\xi = \xi^*$ and in particular

$$\xi|_{y=y_*} = \xi_1|_{y=y_*}, \quad \xi_1|_{y=y_0} = 2\,\xi_1|_{y=y_*}.$$

In Fig. 1 two pairs of rays starting at the point $\xi = 0$, $y_0 = 0.3$ for $\alpha = 0.65$ ($\omega = 0.6$) and $\alpha = 0.45$ ($\omega = 0.75$) are represented. The first pair for $\alpha = 0.65$ consists of the ascending ray OAB (which in turn consists of the incident ray OA and the reflected ray AB) and the descending incident ray OC. The second pair for $\alpha = 0.45$ consists of the ascending ray ODE and the descending incident ray OF. The descending incident rays do not reflect. In the domain $0 < y < y_0$, the reflected field is still described by the integral from (5.5). The field of the descending incident wave is determined by (5.2), where we place the sign "+" at the eikonal $s(y,\omega)$ determined by (5.1).

In Figs. 2 and 3 we represent the family of rays for two values of y_0 : $y_0 = 0.3$ in Fig. 2 and $y_0 = 0.7$ in Fig. 3. There are the ascending rays that have a turning point and the descending ones without a turning point. In Fig. 2 the value of α changes from 0.4 to 1 (which corresponds to a change in ω from 0 to 0.77) with the step 0.1. In Fig. 3 the value of α changes subject to the same limitations, but with the step 0.06. The envelope curve for the rays (the caustic surface) is also represented in the figures. This will be discussed below.

Let us now estimate the fields represented in integral form. We do this by using the example of the incident wave (5.2). Applying the stationary-phase method ($\lambda >> 1$) to the integral, we get

$$w(\xi, y) = \frac{B(\omega, y, y_0, z, z_0)}{\sqrt{\lambda \frac{\partial \xi(y,\omega)}{\partial \omega}}} \cos\left[\lambda\left(\omega\xi - s(y,\omega)\right) + \frac{\pi}{4}\right] \tag{5.7}$$

where $B(\omega, y, y_0, z, z_0) = \frac{4\sqrt{2} y_0 \omega \sin z_0 \sin \frac{z y_0}{y}}{\sqrt{\pi} y \sqrt{1-\omega^2} \sqrt[4]{1-y^2(1-\omega^2)} \sqrt[4]{1-y_0^2(1-\omega^2)}}$, and the function $\xi(y, \omega)$ is determined by (5.3). In the expression (5.7) the frequency $\omega = \omega(\xi, y)$ is implicitly determined for the prescribed values of ξ and y by a solution of the equation

$$\xi = \xi(y, \omega). \tag{5.8}$$

Thus, in order to find, for instance, the incident wave at the prescribed value of y as a function of ξ, we need to solve the determinative equation (5.8) with respect to ω for each value of ξ and then substitute the result in (5.7).

However, there is a possibility to simplify significantly the determination of the field mentioned above. This is done by considering (5.7) as a function of ω only at the prescribed value of y : $w\left(\xi(y,\omega), y\right)$, together with the ray equation $\xi = \xi(y, \omega)$ determined by (5.3); we can easily find the desired functional dependence $w(\xi, y)$ parametrically. This is possible because all functions from the formulae mentioned above are explicit.

Similarly, using the stationary-phase method, we may construct the field of the reflected wave $w_1(\xi, y)$:

$$w_1(\omega, y) = -\frac{B(\omega, y, y_0, z, z_0)}{\sqrt{\lambda \frac{\partial \xi_1(y,\omega)}{\partial \omega}}} \cos\left[\lambda\left(\omega\xi_1(y,\omega) - s_1(y,\omega)\right) + \frac{3\pi}{4}\right], \quad \xi = \xi_1(y, \omega). \tag{5.9}$$

For the incident field $w_2(\xi, y)$ formed by the descending rays and we have

$$w_2(\omega, y) = -\frac{B(\omega, y, y_0, z, z_0)}{\sqrt{\lambda \left(-\frac{\partial \xi(y,\omega)}{\partial \omega}\right)}} \cos\left[\lambda\left(-\omega\xi(y,\omega) + s(y,\omega)\right) + \frac{\pi}{4}\right], \quad \xi = -\xi(y, \omega) \tag{5.10}$$

We note that the radical expression in the denominator of (5.10) is positive, since in the corresponding expression for the eikonal the upper limit of integration is less than the lower one. The amplitudes of the obtained fields at large values of ξ decrease as $\xi^{-1/2}$. This can easily be proved by considering the ray equation for, e.g., the incident wave (5.3). Large values of ξ correspond to small values of α (at the prescribed value of y); then $\xi \sim \alpha^{-3/2}$, and $\xi' \sim \alpha^{-5/2}$. Substituting these estimates in the amplitude of the incident wave, we obtain the desired result.

In Fig. 4 one can see the incident wave $w_2(\xi)$ formed by the ascending rays, the reflected wave $w_1(\xi)$ and the sum of these waves (the integral field). The incident and the reflected waves are obtained by the stationary-phase method (in parametric form) and by numerical integration. The values of the parameters used in the calculations are $\lambda = 16$, $y_0 = 0.3$, $y = 0.95$, $z_0 = 1.57$, $z = 2.32$. One can see in the figure that the frequency and the amplitude of the reflected wave are less than those of the incident wave. This becomes clear from Fig. 2, since the reflected ray coming to the point of intersection of two rays starts at y_0 at a larger angle than the incident ray. Therefore its optical path length is also greater than that of the incident ray. However these frequencies and amplitudes are not too different, which is why in the figure of the integral field we clearly see wave trains (or beatings).

6 The field in the domain of the overcritical velocities ($y > 1$); the caustic surface and the uniform approximation for the integrand

The wave space of solutions in the domain of the overcritical velocities is bounded by the line $y = 1$ and, as one can see in Figs. 2 and 3, by the caustic surface (the envelope curve of the incident ascending rays) [1, Chap. 3]. Therefore, we first describe the behavior of the caustic surface.

The caustic surface is determined by the solution of the system

$$\frac{\partial \xi(y, \alpha)}{\partial \omega} = 0, \quad \xi = \xi(y, \alpha). \tag{6.1}$$

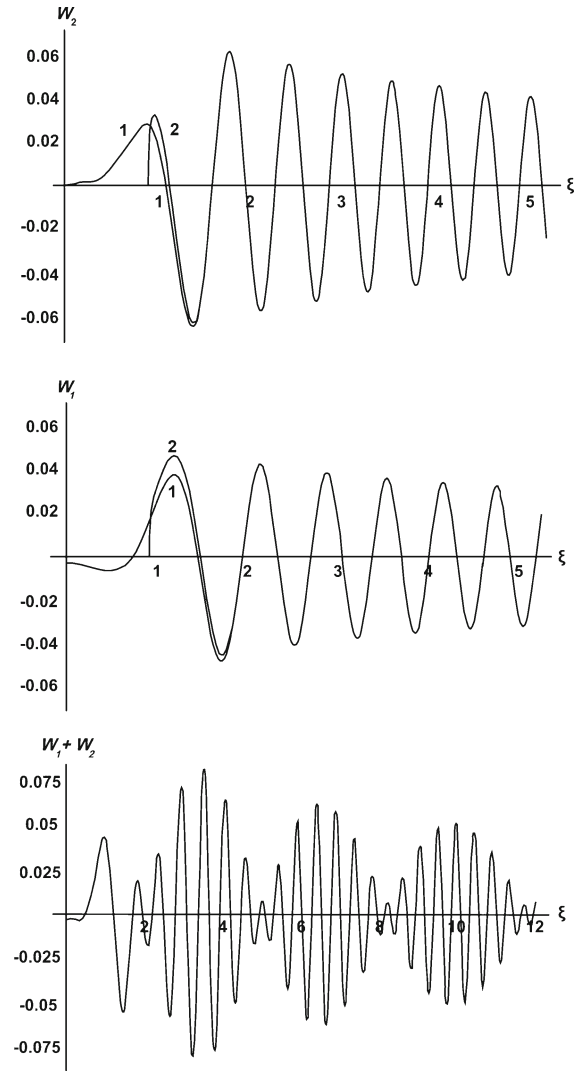

Fig. 4 Vertical component w of the velocity along ξ-axis

Here, since $\alpha = 1 - \omega^2$, the first equation of (6.1) splits into two equations

$$\omega = 0, \quad \frac{\partial \xi(y, \alpha)}{\partial \alpha} = 0.$$

Then we obtain the envelope curve itself from the following system

$$\frac{\partial \xi(y, \alpha)}{\partial \alpha} = 0, \quad \xi = \xi(y, \alpha) \tag{6.2}$$

and the "beak-like" curve formed by the incident and the reflected ray at $\omega = 0 (\alpha = 1)$

$$\xi = \xi(0, y), \quad \xi = \xi_1(0, y), \tag{6.3}$$

where $\xi(\omega, y)$ and $\xi_1(\omega, y)$ are determined by (5.3) and (5.6).

When the value of y is close to 1, the equation for the "beak-like" curve is a semi cubic parabola with the backtracking point $\xi = \xi_0$ and $y = 1$,

$$(\xi - \xi_0)^2 = \frac{8}{9}(1 - y)^3, \tag{6.4}$$

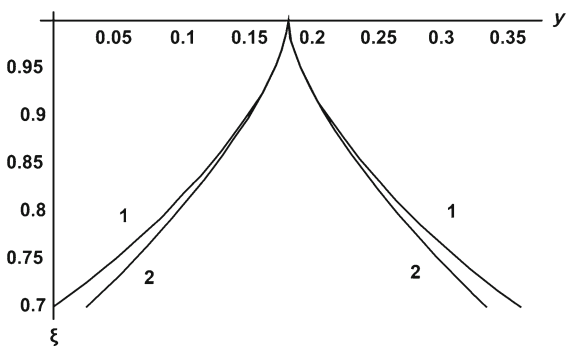

Fig. 5 Caustic curve and its approximation

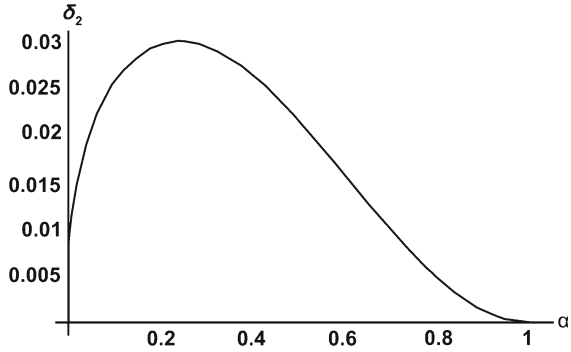

Fig. 6 Correction to the caustic curve

where $\xi_0 = \log\left(1+\sqrt{1-y_0^2}\right) - \sqrt{1-y_0^2} - \log y_0$. In Fig. 5 one can see the "beak" itself (see (6.3)) (line 1) and its approximation (6.4) (line 2) at $y_0 = 0.7$. We notice that the approximation (6.4) depends only on the single parameter y_0 (on the horizon of the source's motion).

Let us now rewrite the first equation of (6.2) in the following form

$$\sqrt{1-y^2\alpha} = \frac{1-\alpha}{\varphi(y,\alpha)}, \tag{6.5}$$

where

$$\varphi(y,\alpha) = \frac{\alpha-1}{\sqrt{1-y_0^2\alpha}} - 3\left(\log y - \log y_0 - \log\left(1+\sqrt{1-y^2\alpha}\right) + \log\left(1+\sqrt{1-y_0^2\alpha}\right)\right).$$

The right-hand term in (6.5) for α close to 1 tends to zero; the function $\varphi(y,\alpha)$ is bounded from below with respect to α. This allows one to apply a perturbation method to (6.5). In the first approximation we obtain its solution substituting zero for the right-hand term in (6.5): $y = \frac{1}{\sqrt{\alpha}}$, or $\alpha = \frac{1}{y^2}$, which together with $\xi = \xi(y,\alpha)$, where $\alpha = 1/y^2$, gives the curve passing through the turning points of the rays:

$$\xi_\pi(y) = -\sqrt{y^2-y_0^2} + y^3 \log\left(\frac{y}{y_0} + \sqrt{\left(\frac{y}{y_0}\right)^2 - 1}\right). \tag{6.6}$$

We obtain the second approximation by substituting the value $1/\sqrt{\alpha}$ for y in $\varphi(y,\alpha)$:

$$y = \frac{1}{\sqrt{\alpha}}\sqrt{1-\delta_2}, \quad \delta_2 = \frac{(1-\alpha)^2}{\varphi^2\left(\frac{1}{\sqrt{\alpha}},\alpha\right)}. \tag{6.7}$$

One can find the graph of the correction for the first approximation δ_2 in Fig. 6. The maximum value of the correction is only 3%.

Equation 6.7 together with $\xi = \xi(y,\alpha)$, where it is needed to substitute for y its value from (6.7), gives the second approximation for the caustic surface in a parametric way. The caustic surface obtained in this approximation is plotted in Figs. 2 and 3.

Describing the field of the vertical velocity in the domain $y > 1$ requires taking into account the turning point $\omega_* = \frac{\sqrt{y^2-1}}{y}$, which is a branch point in the complex plane ω. At this point the amplitude of the integrand is equal to infinity. Therefore one should split the whole interval of integration by ω from 0 to 1 into two intervals: from 0 to ω_*, and from ω_* to 1. The second interval of integration corresponds to the domain to the right of the caustic surface (real rays), the first interval of integration corresponds to the domain to the left of the caustic surface (complex rays). The incident and the reflected fields are still determined by the formulae (5.2) and (5.5), but the lower limit of

integration becomes equal to ω_*. In order to find the integrand on the first interval, i.e., for the field of the so-called penetrating wave, we consider the analytic continuation of the integrand of the incident wave by ω through the lower half-plane (or of the reflected wave through the upper one). In any case, we obtain the following expression for the penetrating wave w_π:

$$w_2 = \mathfrak{Re} \int_0^{\omega_*} \frac{4e^{i\frac{3\pi}{4}} y_0\omega \ \sin z_0 \ \sin\frac{zy_0}{y}}{\pi y\sqrt{1-\omega^2}\left(y^2\alpha-1\right)^{1/4}\left(1-y_0^2\alpha\right)^{1/4}} e^{i\lambda(\omega\xi - s_2(\omega,y))}\, d\omega, \tag{6.8}$$

where

$$s_2(\omega, y) = \frac{\omega}{\sqrt{1-\omega^2}}\left(-i\sqrt{y^2\alpha-1} - \log\left(1-i\sqrt{y^2\alpha-1}\right) + \log y - \sqrt{1-y_0^2\alpha}\right.$$
$$\left. + \log\left(1+\sqrt{1-y_0^2\alpha}\right) - \log y_0\right).$$

Thus, the integral field consists of three components, viz.

$$w_c = w + w_1 + w_2.$$

Let us write the integrand f_c

$$f_c = f + f_1, \quad \text{for } \omega > \omega_*, \quad f_c = f_2, \quad \text{for } \omega < \omega_*, \quad f = \mathfrak{Re}\frac{b(\omega, y)}{\left(1-y^2\alpha\right)^{1/4}} e^{i\left(\lambda(\omega\xi - s(\omega,y)) + \frac{\pi}{2}\right)},$$

$$f_1 = \mathfrak{Re}\frac{b(\omega, y)}{\left(1-y^2\alpha\right)^{1/4}} e^{i(\lambda(\omega\xi - s_1(\omega,y)) + \pi)}, \quad f_2 = \mathfrak{Re}\frac{b(\omega, y)}{\left(y^2\alpha-1\right)^{1/4}} e^{i\left(\lambda(\omega\xi - s_2(\omega,y)) + \frac{3\pi}{4}\right)},$$

$$b(\omega, y) = \frac{4y_0\omega \ \sin z_0 \ \sin\frac{zy_0}{y}}{\pi y\sqrt{1-\omega^2}\left(1-y_o^2\alpha\right)^{1/4}}. \tag{6.9}$$

The functions f, f_1 and f_2 are the elementary solutions of the internal gravity equation (3.3) at the prescribed value of the frequency ω in the WKB approximation (geometrical optics) or, what is the same, the elementary WKB solutions.

Our goal is to find a function $G(\omega, \xi, y)$ that it is regular at the point $\omega = \omega_*$ and its asymptotic form for large λ coincides with the asymptotic form of the function f_2 to the left from the turning point and with $f + f_1$ to the right of the turning point:

In order to do so we introduce the following function

$$\Delta(\omega, y) = S(y_\pi, \omega) - S(y, \omega), \quad \Delta(\omega, y) = \frac{\omega}{\sqrt{\alpha}}\left(\log\frac{1}{\sqrt{\alpha}} - \sqrt{1-y^2\alpha} + \log\left(1+\sqrt{1-y^2\alpha}\right) - \log y\right), \tag{6.10}$$

which represents the phase incursion from the point y to the turning point $y_\pi = \frac{1}{\sqrt{\alpha}}$. We expand $\Delta(\omega, y)$ in the series with respect to the argument $\Omega = \alpha y^2$, supposing that Ω is close to 1, and take only the dominant term of the series,

$$\tilde{\Delta} = \frac{\omega}{\sqrt{\alpha}} \frac{\sqrt{1-y^2\alpha}^3}{3}. \tag{6.11}$$

We rewrite the expression (6.9), factoring out the common factor

$$i\varphi(\omega, \xi) = i\left(\lambda\left(\omega\xi - s(y_\pi, \omega)\right) + \frac{3\pi}{4}\right), \quad f = b(\omega, y)e^{i\varphi(\omega,\xi)}\frac{e^{i\left(\lambda\tilde{\Delta} - \frac{\pi}{4}\right)}}{\sqrt[4]{1-y^2\alpha}},$$

$$f_1 = b(\omega, y)e^{i\varphi(\omega,\xi)}\frac{e^{-i\left(\lambda\tilde{\Delta} - \frac{\pi}{4}\right)}}{\sqrt[4]{1-y^2\alpha}}, \quad f_2 = b(\omega, y)e^{i\varphi(\omega,\xi)}\frac{e^{-\lambda\left|\tilde{\Delta}\right|}}{\sqrt[4]{y^2\alpha-1}}. \tag{6.12}$$

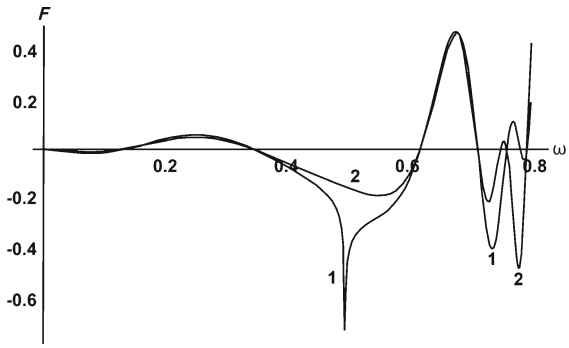

Fig. 7 The local asymptotic and the WKB approximation of the vertical velocity component w integrand for $y > 1$

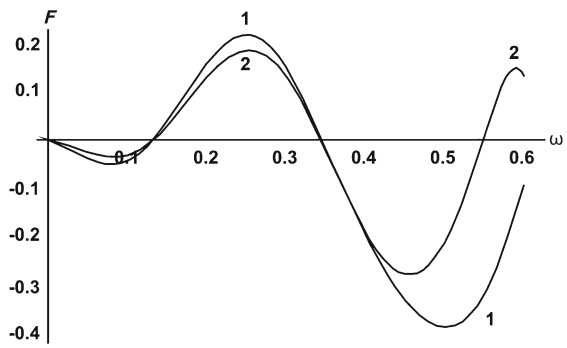

Fig. 8 The local asymptotic and the WKB approximation of the vertical velocity component w integrand for $y < 1$

It is easy to verify that the formulae (6.12) and (6.11) represent the asymptotic form of the following function

$$\tilde{G}(\omega, \xi, y) = 2\sqrt{\pi}\cos(\varphi(\omega, \xi))\, b(\omega, y) q^{1/6} \mathrm{Ai}\left(q^{2/3}(1 - y^2\alpha)\right), \tag{6.13}$$

$$q = \frac{\lambda\omega}{2\sqrt{1-\omega^2}}, \quad \mathrm{Ai}(x) = \frac{1}{2\pi}\int_{-\infty}^{\infty} \mathrm{e}^{\mathrm{i}\left(\frac{t^2}{3} - xt\right)}\mathrm{d}t$$

where $\mathrm{Ai}(x)$ is the Airy function [13, Chap. 9].

The function $\tilde{G}$ is the local asymptotic form, i.e., it describes the solution near the turning point $\omega = \omega_*$. It is easy to verify that the expression (6.12) is the asymptotic form of the function $\tilde{G}(\omega, \xi, y)$. Therefore it will suffice to consider the asymptotic form of the Airy function [13, Chap. 9]

$$\mathrm{Ai}(x) \sim \frac{1}{\sqrt{\pi}x^{1/4}}\cos\left(\frac{2}{3}x^{3/2} - \frac{\pi}{4}\right) \quad \text{when } x \to +\infty, \quad \mathrm{Ai}(x) \sim \frac{1}{2\sqrt{\pi}\,|x|^{1/4}}\,\mathrm{e}^{-\frac{2}{3}|x|^{3/2}} \quad \text{when } x \to -\infty$$

We notice that the asymptotic form (6.13) also holds in the domain of the subcritical velocities ($y < 1$), when there are no turning points in the domain of integration.

In Fig. 7 we represent the function $\tilde{G}(\omega, \xi, y)$ (line 2) and the WKB-solution (6.9) $f + f_1$ (line 1) to the right of the turning point, and f_2 to the left of it (line 1), in the domain $y > 1$ ($y = 1.15$). In Fig. 8 the function $\tilde{G}(\omega, \xi, y)$ (line 2) and the WKB-solution (only $f + f_1$) (line 1) in the domain $y < 1 (y = 0.8)$ are represented. In both cases $\xi = 2$.

The uniform asymptotic form of $\tilde{G}(\omega, \xi, y)$ has the following form

$$\tilde{G}(\omega, \xi, y) = \frac{2\sqrt{\pi}b(\omega, y)\cos(\varphi(\omega, y))\left(\frac{3}{2}\Delta(\omega, y)^{1/6}\right)}{\sqrt{1-y^2\alpha}}\mathrm{Ai}\left(\left(\frac{3}{2}\Delta(\omega, y)\right)^{2/3}\right), \tag{6.14}$$

where $\Delta(\omega, y)$ is determined by (6.10).

We emphasize that the uniform asymptotic form (6.14) at small values of arguments of the Airy function is transformed to the local asymptotic form (6.13), and at large values of the arguments it is transformed to the WKB expansion (6.9) [2, Chap. 5]. The uniform asymptotic form also holds in the domain of subcritical velocities ($y < 1$). It is clear that when $y < y_0$ the incident (descending) wave must be found from the other formulae.

In Fig. 9 we represent the uniform asymptotic form (line 2) and the WKB solution (line 1) at the prescribed $y = 1.15$ ("section" by ω), and in Fig. 10 we represent the uniform asymptotic form (line 2) and the WKB solution (line 1) at the prescribed $\omega = 0.4$ ("section" by y). In Fig. 11 the uniform asymptotic form (line 2) and the WKB solution (line 1) are represented at $y = 0.85$ (the domain of subcritical velocities), i.e., in the case of the absence of turning points. In all figures $\xi = 2$. In all cases one can clearly see the excellent agreement of the uniform asymptotic form and the WKB approximations.

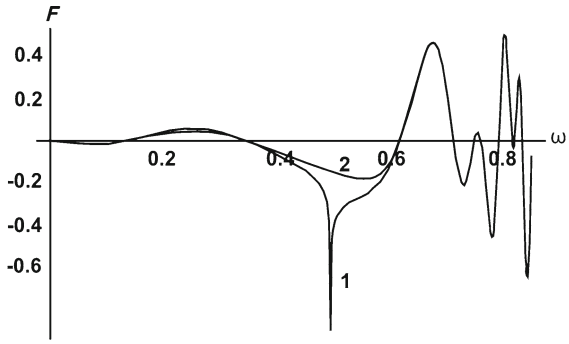

Fig. 9 The uniform asymptotic and the WKB approximation of the vertical component velocity w integrand along the ω-axis and constant y in the domain of critical velocities

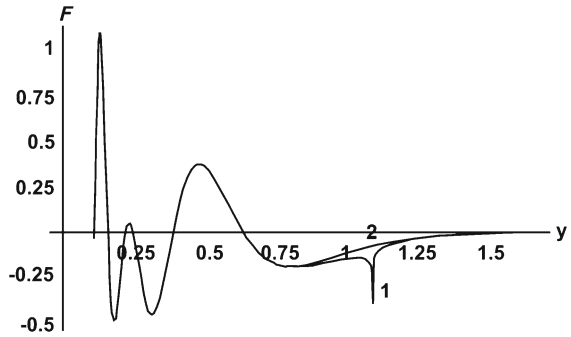

Fig. 10 The uniform asymptotic and the WKB approximation of the vertical velocity component w integrand along y-axis and constant ω

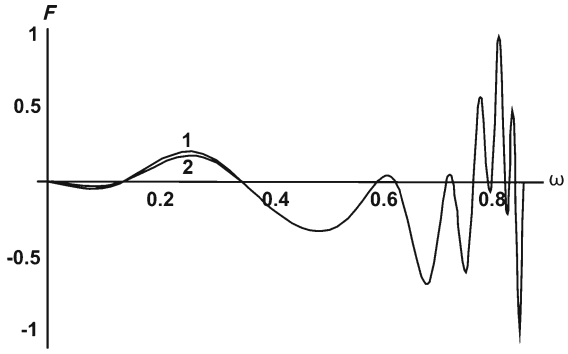

Fig. 11 The uniform asymptotic and the WKB approximation of the vertical velocity component w integrand along the ω-axis and constant y in the domain of subcritical velocities

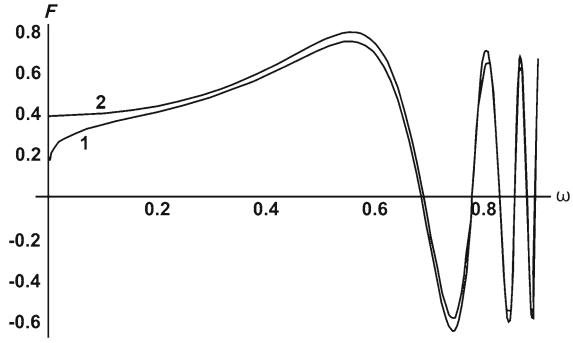

Fig. 12 The uniform Airy and parabolic-cylinder approximations of the vertical velocity component w integrand without the amplitude factors

The uniform asymptotic form describes the integrand of solution w in the domain $y > y_0$ at any values of ω, except in the vicinity of the point $\omega = 0$, $y = 1$ (on the plane ξ, y this is the vicinity where the "beak" sharpens). The argument of the Airy function is not an analytic function for small values of ω (it behaves like $\omega^{2/3}$), and the amplitude behaves like $\omega^{7/6}$. Let us determine the behavior of the integrand at $y = 1$ and for any values of ω. One can find the acceptable function which coincides with the uniform Airy function at large values of ω and which is an analytic function for small values of ω, in the following form

$$F(\omega) = b(\omega, 1)\frac{\Delta^{1/8}(\omega, 1)D\left(\frac{1}{4}, \Delta^{1/4}(\omega, 1)\right)}{\sqrt{\omega}}, \quad D(\nu, x) = \frac{1}{\pi}\mathfrak{Re}\, e^{-ix^4}\int_0^\infty \frac{e^{i(t-x^2)^2}}{t^\nu}dt. \tag{6.15}$$

$D(\nu, x)$ is related to the function of the parabolic cylinder [13, Chap. 8]. In Fig. 12 one can find the integrand (without the amplitude $b(\omega, y)$), which is the uniform Airy function (line 1) and determined by formula (6.15) (line 2). It is clear that the graphs differ only in a very narrow region adjacent to $\omega = 0$.

In Fig. 13 we represent the same graphs but with the amplitude factors $b(\omega, y)$ and $b(\omega)$. It is clear that these graphs almost coincide. Hence, the uniform Airy function can be further applied to the integration by ω. The integral field is determined by integration of the uniform Airy function with respect to ω. In Fig. 14 the integral field w obtained by integration of the WKB approximation is represented. In Fig. 15 one can find the field w obtained by integration of the uniform Airy asymptotic form. We see the complete coincidence of phases and the substantial divergence of the amplitudes. This results from the fact that, as was mentioned above, the WKB solution is equal

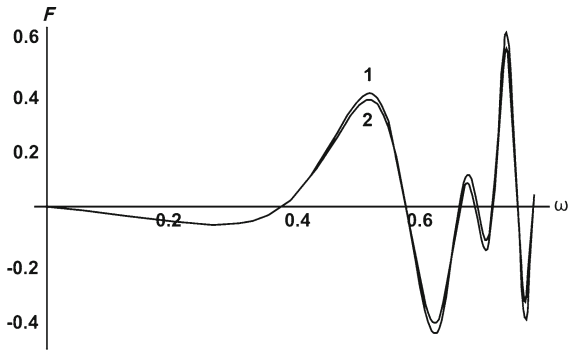

Fig. 13 The uniform Airy and parabolic cylinder approximations of the vertical velocity component w integrand with the amplitude factors

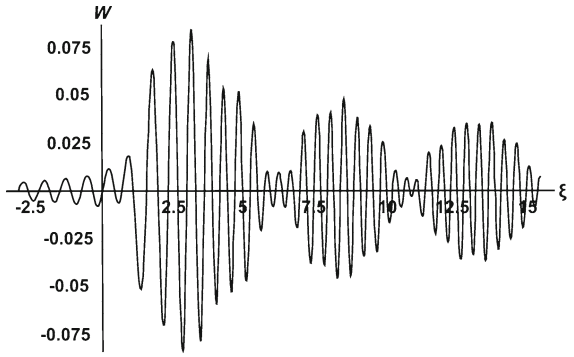

Fig. 14 Vertical component w of the velocity along the ξ-axis calculated by using the WKB approximation

Fig. 15 Vertical component w of the velocity along the ξ-axis calculated by using the uniform Airy approximation

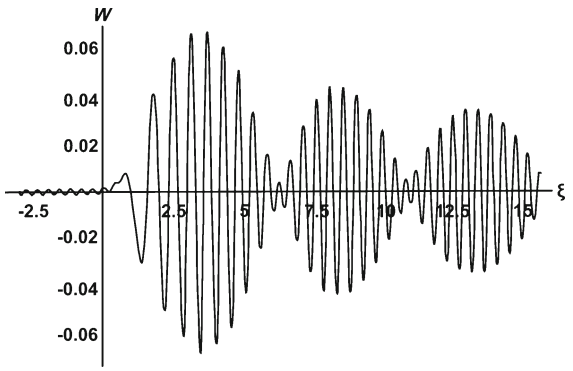

to infinity at the turning point. Despite the integrability of this singularity, the integral of the Airy function over the infinite interval and the integral of its asymptotic form over the same interval differ by approximately 23%. The wave propagating forwards in Fig. 14 is not valid from a physical point of view (it is absent in Fig. 15). This wave emerges due to the contribution of the border set of the integration domain (the turning point) to the integral. In Fig. 16 we see the field w obtained by the integration of the WKB approximation. In Fig. 17 we represent the field w obtained by integration of the uniform Airy asymptotic form.

7 Discussion

The asymptotic representations constructed above allow one to describe the far field of the internal gravity waves generated by a source moving over a slowly varying bottom topography. The obtained asymptotic expressions for the solution are uniform and reproduce the essential features of wave fields near caustic surfaces and wave fronts. In the paper the problem of reconstructing non-harmonic wave packets of the internal gravity waves generated by a source moving in a horizontally stratified medium has been considered. A solution was proposed in terms of modes, propagating independently at the adiabatic approximation, and described as a non-integral-degree series of a small parameter characterizing the stratified medium. In this study we have analyzed the evolution of non-harmonic wave packets of internal gravity waves generated by a moving source under the assumption that the parameters of a vertically stratified medium (e.g. an ocean) vary slowly in the horizontal direction, as compared to the characteristic length of the density. A specific form of the wave packets, which can be parameterized in terms of model functions,

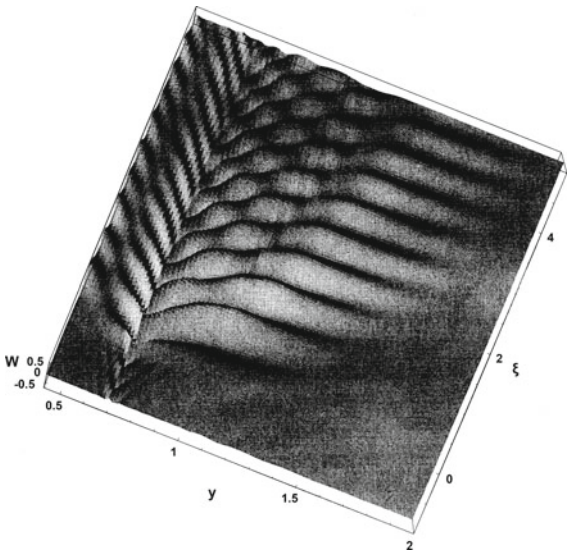

Fig. 16 Vertical component w of the velocity in the (ξ, y)-plane, calculated by using the WKB approximation

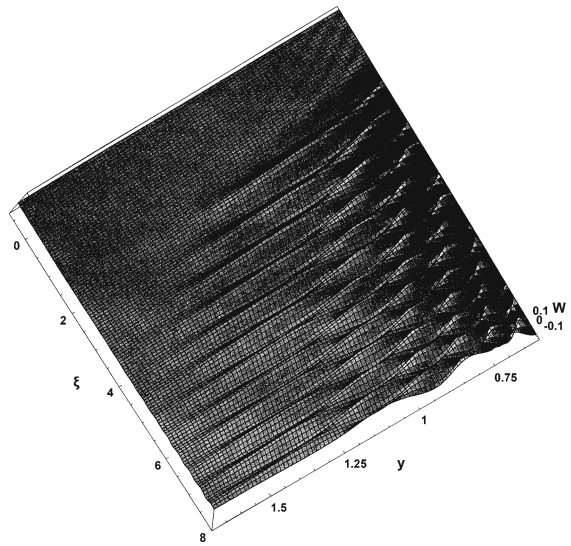

Fig. 17 Vertical component w of the velocity in the (ξ, y)-plane, calculated by using the uniform Airy approximation

e.g. Airy functions, depends on the local behavior of the dispersion curves of individual modes in the vicinity of corresponding critical points.

In this paper the modified space–time ray method was proposed, which belongs to the class of geometrical-optics methods. The key point of the proposed technique is the possibility to derive the asymptotic representation of the solution in terms of a non-integral-degree series of the small parameter $\varepsilon = \Lambda/L$, where Λ is the characteristic wave length, and L is the characteristic scale of the horizontal heterogeneity. The explicit form of the asymptotic solution was determined on the basis of the principles of locality and asymptotic behavior of the solution in case of a stationary and horizontally homogeneous medium. The wave-packet amplitudes are determined from the energy conservation laws along the characteristic curves. A typical assumption made in studies on internal wave evolution in stratified media is that the wave packet is locally harmonic. A modification of the geometrical-optics method, based on an expansion of the solution by model functions, allows us to describe the wave-field structure both far from and in the vicinity of the wave front.

Using the asymptotic representation of the wave field at a large distance from a source moving in a layer of constant depth, we have solved the problem of constructing the uniform asymptotics of the internal waves in a medium of varying depth. The solution was obtained by modifying the previously proposed "vertical modes-horizontal rays" method, which avoids the assumption that the medium parameters vary slowly in a vertical direction. The solution is parameterized through the Airy waves. This allows to describe not only the evolution of the non-harmonic wave packets propagating over a slowly varying fluid bottom, but also specify the wave-field structure associated with an individual mode both far from and close to the wave front of the mode. The Airy-function argument is determined by solving the corresponding eikonal equations and finding vertical spectra of the internal gravity waves. The wave-field amplitude was determined using the energy-conservation law, or another adiabatic invariant, characterizing wave propagation along the characteristic curves.

Modeling typical shapes and stratification of the ocean shelf, we obtained analytic expressions describing the characteristic curves and examined the characteristic properties of the wave-field phase structure. As a result it was possible to observe some peculiarities in the wave-field structure, depending on the shape of the ocean floor, water stratification and the trajectory of a moving source. In particular, we analyzed a spatial blocking effect of the low-frequency components of the wave field, generated by a source moving alongshore with a supercritical velocity. Numerical analyses that were performed using typical ocean parameters reveal that actual dynamics of the

internal gravity waves are strongly influenced by horizontal inhomogeneity of ocean bottom. Here we have used an analytical approach, which avoids the numerical calculation widely used in analysis of internal gravity-wave dynamics in a stratified ocean.

In this paper we have investigated problems in wave theory by means of geometrical-optics methods (WKB method) and its modification. The main question consists in finding an asymptotic solution near a special curve (or surface), which is called a caustic. It is well known, that a caustic is an envelope of a family of rays, and an asymptotic solution is obtained along these rays. Each point of the caustic corresponds to a specified ray, and that ray is tangent at this point.

It is a general rule that a caustic of a family of rays singles out an area in space, so that rays of that family cannot appear in the marked area. There is also another area, and each point of this area has two rays, that pass through this point. One of those rays has already passed this point, and another is going to pass the point. Formal approximation of geometrical optics or WKB approximation cannot be applied near a caustic, because rays merge together in that area, after they were reflected by the caustic. If we want to find a wave field near the caustic, then it is necessary to use a special approximation of the solution, and in the paper a modified ray method was proposed to build an uniform asymptotic expansion of integral forms of the internal gravity-wave field.

After the rays were reflected by the caustic, there is a leap of phase. It is clear that a phase leap can only happen in the area, where methods of geometrical optics, which were used in previous sections, cannot be applied. If the rays touch a caustic several times, then additional phase shifts will result. A phase shift, which was created by a caustic, is rather small in comparison with the change in phase along the ray. But this shift can considerably affect the interference pattern of the wave field.

The results of this paper are of significant interest in physics and mathematics. Apart from that interest, the asymptotic solutions, which were obtained in this paper, can be quite important for engineering applications, since the method of geometrical optics which was modified to calculate the wave field near a caustic, makes it possible to describe different wave fields in a rather big class of other problems.

References

1. Babich VM, Buldyrev VS (2007) Asymptotic methods in short-wavelength diffraction theory. Alpha Science, Oxford
2. Borovikov VA (1994) Uniform stationary phase method. IEE electromagnetic waves, series 40. Institution of Electrical Engineers, London
3. Brekhovskikh LM, Goncharov VV (1994) Mechanics of continua and wave dynamics, 2nd edn, updated. Springer Verlag, Berlin
4. Bulatov VV, Vladimirov YuV (2006) General problems of the internal gravity waves linear theory. http://arxiv.org/abs/physics/0609236
5. Bulatov VV, Vladimirov YuV (2006) Dynamics of the internal gravity waves in the heterogeneous and nonstationary stratified mediums. http://arxiv.org/abs/physics/0611040
6. Bulatov VV, Vladimirov YuV (2007) Internal gravity waves: theory and applications. Nauka Publishers, Moscow
7. Gitterman M (2007) Hydrodynamics of compressible liquids: influence of the piston effect on convection and internal gravity waves. Physica A 386:1–11
8. Gray EP, Hart RW, Farrel RA (1983) The structure of the internal wave Mach front generated by a point source moving in a stratified fluid. Phys Fluids 10:2919–2931
9. Keller JB, Munk WH (1970) Internal wave wakes of a body moving in a stratified fluid. Phys Fluids 6:1425–1431
10. Keller JB, Van Mow C (1969) Internal wave propagation in a inhomogeneous fluid of non-uniform dept. J Fluid Mech 2:365–374
11. Keller JB, Levy DM, Ahluwalia DS (1981) Internal and surface wave production in a stratified fluid. Wave Motion 3:215–229
12. Lighthill MJ (1978) Waves in fluids. Cambridge University Press, Cambridge
13. Luke YL (1975) Mathematical functions and their approximation. Academic Press Inc, New York
14. Miles JW, Chamberlain PG (1998) Topographical scattering of gravity waves. J Fluid Mech 361:175–188
15. Miropol'skii YuZ, Shishkina OV (2001) Dynamics of internal gravity waves in the ocean. Kluwer Academic Publishers, Boston
16. Morozov EG (1995) Semidiurnal internal wave global field. Deep Sea Res 42:135–148
17. Voisin B (1994) Internal wave generation in uniformly stratified fluids. Part II. Moving point sources. J Fluid Mech 261:333–374
18. Wunsch C (1968) On the propagation of internal waves up a slope. Deep Sea Res 15:251–258